JOURNAL OF VIROLOGY, May 1997, p. 3603–3612 Vol. 71, No. 5
0022-538X/97/$04.00+0

Study of Herpes Simplex Virus Maturation during a Synchronous Wave of Assembly

GEOFFREY A. CHURCH AND DUNCAN W. WILSON*

Department of Developmental and Molecular Biology, Albert Einstein College of Medicine, New York, New York 10461

Received 30 October 1996/Accepted 5 February 1997

Production of an infectious herpes simplex virus (HSV) particle requires sequential progression of maturing virions through a series of complex assembly events. Capsids must be constructed in the nucleus, packaged with the viral genome, and transported to the nuclear periphery. They then bud into the nuclear membrane to acquire an envelope, traffic through the cytoplasm, and are released from the cell. Most of these phenomena are very poorly defined, and no suitable model system has previously been available to facilitate molecular analyses of genomic DNA packaging, capsid envelopment, and intracellular virion trafficking. We report the development of such an assay system for HSV type 1 (HSV-1). Using a reversible temperature-sensitive mutation in capsid assembly, we have developed conditions in which an accumulated population of immature capsids can be rapidly, efficiently, and synchronously chased to maturity. By assaying synchronized scaffold cleavage, DNA packaging, and acquisition of infectivity, we have demonstrated the kinetics with which these events occur. Kinetic and morphological features of intranuclear and extranuclear virion trafficking have similarly been examined by indirect immunofluorescence microscopy and electron microscopy. This system should prove a generally useful tool for the molecular dissection of many late events in HSV-1 biogenesis.

The biogenesis and intracellular trafficking of herpes simplex virus (HSV) are complex and poorly understood events. HSV assembly begins in the infected-cell nucleus with the construction and maturation of the viral capsid. An early intermediate in this process is believed to be the large-cored B capsid (29, 38), which contains an electron-translucent inner shell composed of several related polypeptides (8, 20, 25, 28). The most abundant core component is ICP35 (26), present at about 1,100 copies per capsid and thought to be analogous to the scaffold protein of double-stranded DNA bacteriophage (7). Full-length ICP35, termed ICP35c,d, is modified to ICP35e,f by proteolytic cleavage of its 25 carboxy-terminal amino acids (4, 18–20). The protease responsible is the product of the HSV UL26 gene, and UL26 inactivation blocks capsid maturation (11, 29). ICP35c,d cleavage correlates with condensation of the inner shell to generate small-cored B capsids (29, 38) and is also required for maturation of the outer shell, since the major capsid protein VP5 fails to display certain epitopes if ICP35 cleavage is blocked (11, 21, 22). Small-cored B capsids are probably able to package the viral genome, resulting in expulsion of the scaffold core (13, 32) and the formation of C capsids, which contain an irregular electron-dense center. Mature C capsids bud into the inner nuclear membrane and acquire a lipid envelope (33).

Little is known concerning the kinetics or molecular details of viral DNA packaging, capsid-nuclear membrane interaction, or capsid envelopment. Subsequent events in HSV biogenesis are equally obscure. One view is that enveloped virions accumulate in the perinuclear space, then move via vesicular transport to the Golgi complex, and are eventually secreted from the cell (6, 10, 33). Alternatively, Stackpole (37) suggested that perinuclear virions catalyze fusion of their envelopes with the outer nuclear or endoplasmic reticulum membrane, releasing naked capsids into the cytoplasm. These capsids must subsequently reenvelope by budding into the lumen of a cytoplasmic organelle such as the Golgi apparatus (40). Similar egress pathways have been proposed for other herpesviruses (12, 24, 43). In support of this model, retention of a viral glycoprotein in the nuclear membranes and endoplasmic reticulum prevents its incorporation into the envelopes of secreted virions (5). Also consistent with the reenvelopment model is the presence of naked extranuclear capsids in infected cells (27, 43), but it has been suggested that these capsids may represent a "dead-end," nonproductive population which has erroneously and irreversibly de-enveloped (6, 33). In summary, the pathway of viral trafficking within and egress from cells, the rate at which capsids travel from the nucleus to cell periphery, and the rate of formation (and significance) of naked cytoplasmic capsids all remain unknown.

A serious obstacle to the study of HSV assembly and egress is that all viral maturation and trafficking intermediates exist simultaneously within infected cells. This makes it extremely difficult to define not only the sequence of events in HSV assembly but also their kinetics. The ability to follow a single population of virions as they assemble and traffic in a synchronous wave would be an important tool in the molecular dissection of HSV biogenesis.

Here we report the establishment and initial characterization of such a synchronous assay system. Using a reversible temperature-sensitive defect in capsid assembly, we have established conditions in which an accumulated population of HSV matures, becomes packaged, envelopes, and acquires infectivity in a single, near-synchronous wave. By monitoring the fate of this synchronous population, we have obtained data concerning the kinetics of scaffold cleavage, DNA packaging, infectious virion production, and intracellular viral trafficking. It is anticipated that this assay will provide a useful model system for the study of many late events in HSV biogenesis.

* Corresponding author. Mailing address: Department of Developmental and Molecular Biology, Albert Einstein College of Medicine, 1300 Morris Park Ave., Bronx, New York, NY 10461. Phone: (718) 430-2305. Fax: (718) 430-8567. E-mail: wilson@aecom.yu.edu.

MATERIALS AND METHODS

Viruses and cells. African green monkey kidney (Vero) cells were grown in DMEM-NCS-PS (Dulbecco modified Eagle medium supplemented with 10%

newborn calf serum and 1% penicillin-streptomycin) (GIBCO Laboratories). HSV *ts*Prot.A, derived from strain KOS1.1 as previously described (11), was a kind gift from Min Gao and Richard J. Colonno (Bristol-Myers Squibb Pharmaceutical Research Institute). Stocks of *ts*Prot.A and the wild-type strain SC16 were grown by low-multiplicity passage on Vero cells at 31 and 36°C, respectively. Titers were determined by plaque assay on preformed Vero monolayers at 31 or 36°C (titers of *ts*Prot.A were identical at both temperatures).

Time courses of PFU production. Vero cells were infected with HSV at a multiplicity of infection of 10 in DMEM-NCS-PS for 1 h at 37°C, then (with chilled solutions) washed in phosphate-buffered saline (PBS), treated for 0.5 min with 135 mM NaCl-10 mM KCl–100 mM glycine, pH 3.0 (to inactivate unpenetrated virus), returned to neutral pH by washing the cells with PBS and then with a 1:1 mixture of PBS-DMEM, and finally overlaid with prewarmed DMEM-NCS-PS. Infected cells were either collected immediately or incubated for various times at 39 or 36°C. Temperature downshifts were accomplished by transferring dishes of infected cells to shallow trays of water in a 31°C gassed incubator. The dishes were transferred to a prechilled metal surface in a −20°C freezer at various time points. To determine PFU yields, the cells were thawed, collected by scraping, and sonicated and the resulting extract was titrated onto preformed Vero cell monolayers.

Analysis of viral DNA. Cells were infected, acid washed, and incubated as described above for PFU production, except that the multiplicity of infection was 3. Total infected-cell DNA was prepared by a modification of the method of Shao and colleagues (34). Cells were rinsed with prechilled Tris-buffered saline (TBS; 130 mM NaCl–20 mM KCl–25 mM Tris-Cl, pH 7.4), then frozen, thawed, sonicated, and digested with 100 μg of proteinase K (Sigma Chemical Co.) per ml in the presence of TBS containing 0.4% sodium dodecyl sulfate (SDS) for 3 h at 37°C. Pancreatic RNase A (Sigma Chemical Co.) was added to a final concentration of 100 μg/ml, and incubation continued for a further 30 min before exhaustive phenol and chloroform extractions followed by ethanol precipitation. DNA was digested to completion with the restriction endonuclease *Bam*HI, subjected to electrophoresis on a 1.0% agarose gel, and blotted to a nylon membrane (Schleicher and Schuell). The membrane was hybridized with a ^{32}P-radiolabelled DNA probe prepared by random hexanucleotide priming from a mixture of two different DNA fragments: one bridging the SQ cleavage junction (kindly provided by Sandra K. Weller, University of Connecticut Health Center) and another derived from the UL22 gene. Following hybridization, the filter was exposed to DuPont X-ray film.

Western blotting. Cells were infected and samples were taken as described above for DNA analysis. After the cells were freeze-thawed and sonicated, extracts were heated in Laemmli buffer at 65°C for 5 min and then subjected to denaturing SDS-polyacrylamide gel electrophoresis (SDS-PAGE) with a 12.5% polyacrylamide gel. Proteins were transferred to a nitrocellulose filter at 125 mA for 2 h with a Hoffer semidry blotter, and the filter was incubated overnight in blocking buffer (PBS–0.1% Tween 20–5% dried milk) at 4°C. The filter was probed for 2 h at room temperature with a 1:1,000 dilution of the mouse monoclonal antibody MCA406 (Serotec) in blocking buffer and washed for 20 min with four changes of PBS–0.1% Tween 20. After a 1-h incubation with peroxidase-conjugated goat anti-mouse immunoglobulin G (Sigma Chemical Co.) diluted 1:2,000 in blocking buffer, the filter was washed as described above, treated for 1 min with chemiluminscence reagent (DuPont-NEN), and exposed to X-ray film.

Indirect immunofluorescence microscopy. Vero cells were grown to 90% confluence on glass coverslips and then infected with HSV at a multiplicity of 10 for 1 h at 37°C. The medium was replaced, and infection was allowed to continue at 36 or 39°C for 6.5 h. Cycloheximide was added to a final concentration of 20 μg/ml, and incubation continued for 30 min before transfer to a 31°C water bath. At specific times after temperature downshift, coverslips were processed for indirect immunocytochemistry as follows (all procedures were performed at room temperature). Cells were rinsed in PBS, fixed in PBS–2% paraformaldehyde–0.2% glutaraldehyde for 10 min, and made permeable by immersion in PBS–0.1% Triton X-100 for 10 min, and fixative was quenched by incubation with a 1-mg/ml sodium borohydride-PBS solution for 15 min. Samples were incubated for 30 min with blocking buffer (PBS–20% NCS) and then for 1 h with anti-VP5 monoclonal antibody 6F10 or 8F5 (kindly provided by Jay Brown, University of Virginia) diluted in blocking buffer. After four 5-min washes with PBS, cells were incubated for 1 h with Texas Red-conjugated goat anti-mouse antibody (Southern Biotechnology Associates), washed with PBS as described above, and mounted by using a 25-mg/ml solution of 1,4,-diazabicyclo(2,2,2) octane (DABCO; Sigma Chemical Co.) in PBS–50% glycerol. Specimens were examined with a Biorad MRC 600 scanning laser confocal microscope.

Electron microscopy. Vero cells were grown in 6-cm-diameter tissue culture dishes and then infected with HSV *ts*Prot.A, and temperature was shifted in the presence of cycloheximide exactly as described above for indirect immunofluorescence microscopy. At appropriate times, cells were rinsed in PBS, fixed in 2.5% glutaraldehyde–0.1 M sodium cacodylate for 45 min, rinsed in 0.1 M sodium cacodylate, postfixed in 1% osmium tetroxide–0.1 M sodium cacodylate, stained in 1% uranyl acetate, dehydrated, and embedded.

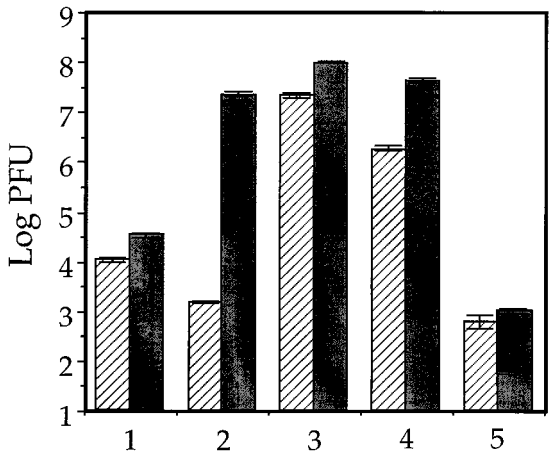

FIG. 1. *ts*Prot.A matures to infectivity following temperature downshift. Vero cells were infected with *ts*Prot.A (hatched bars) or SC16 (shaded bars), acid washed to inactivate residual input virus, and then harvested immediately or incubated under a variety of conditions. Extracts were prepared and titrated for levels of PFU production. The values plotted are the means of four samples, and error bars indicate the standard deviations from the means. Cells were harvested immediately after acid wash (bars 1) or incubated for 7 h at 39°C (bars 2) and then for 3 h at 31°C (bars 3, 4, and 5). Cycloheximide (20 μg/ml) was added 0.5 h before the start of the 31°C (bars 4) or 39°C (bars 5) incubation. All extracts were adjusted to the same cycloheximide concentration before titration.

RESULTS

Synchronized *ts*Prot.A can mature to infectivity in the absence of new protein synthesis. The viral strain *ts*Prot.A (11) carries a thermolabile defect within the UL26-encoded maturational protease. This UL26 allele, originally generated and characterized in the context of HSV strain *ts*1201 (29), results in the accumulation of uncleaved ICP35c,d and large-cored B capsids at the nonpermissive temperature of 39°C. Importantly, this phenotype was shown to be at least partially reversible: upon return to the permissive temperature, ICP35c,d cleavage and DNA packaging resumed even in the presence of cycloheximide (1, 29, 32). We wished to determine whether *ts*Prot.A, arrested at the point of the 39°C block, could subsequently mature to infectivity, providing a model system for HSV assembly.

To test this, Vero cells were infected with *ts*Prot.A or the wild-type virus strain SC16, and after 1 h, residual input virus was inactivated by acid wash. Infected cells were incubated under various conditions, extracts were prepared, and levels of progeny PFU were determined by plaque titration. Figure 1 shows that after 7 h of incubation at 39°C, SC16 PFU yields had increased by about 3 log units over levels of surviving input virus (compare shaded bars 1 and 2). In contrast, *ts*Prot.A failed to replicate at the nonpermissive temperature, and PFU yields were below background (hatched bars 1 and 2). Following downshift to 31°C for 3 h, SC16 PFU numbers increased about fivefold; in contrast, the yields of infectious *ts*Prot.A increased about 10,000-fold (bar 3). Three log units of this increase resulted from maturation of pre-existing polypeptides rather than de novo protein synthesis, as shown by the addition of 20 μg of cycloheximide per ml 30 min prior to the 31°C temperature shift (bar 4). The cycloheximide used in this experiment was sufficient to block new protein synthesis, since it prevented any PFU production when added immediately postinfection to cells subsequently incubated at 39°C for 7 h and then at 31°C for 3 h (bar 5). The results of these experiments suggest that accumulated immature *ts*Prot.A virions are

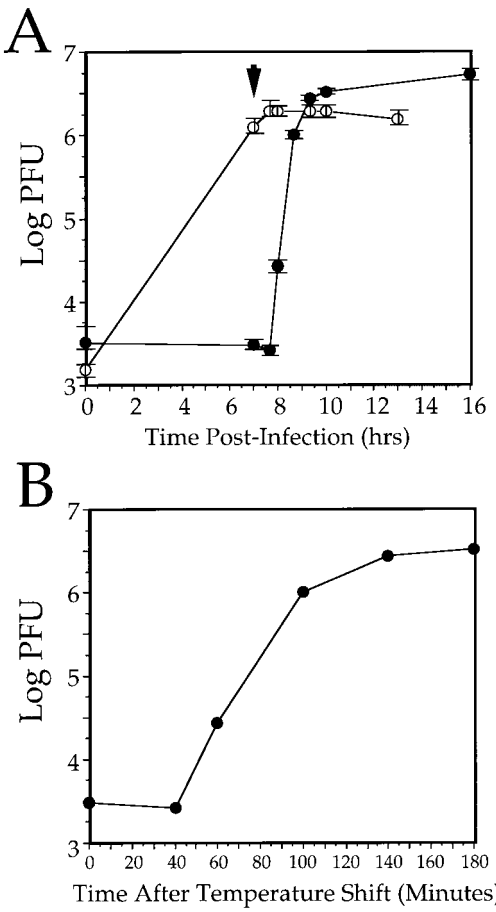

FIG. 2. Kinetics of maturation to infectivity. Cells were infected with *ts*Prot.A (solid circles) or SC16 (open circles), acid washed, and incubated at 39°C. After 6.5 h, cycloheximide was added, and after another 30 min, the incubation temperature was downshifted to 31°C. Extracts were prepared at various time points and titrated to determine PFU yield. The values plotted are the means of four samples, and error bars indicate the standard deviations from the means. (A) Entire time course of incubation. The arrowhead indicates the time of downshift to 31°C. (B) Expansion of *ts*Prot.A data to show kinetics of PFU production.

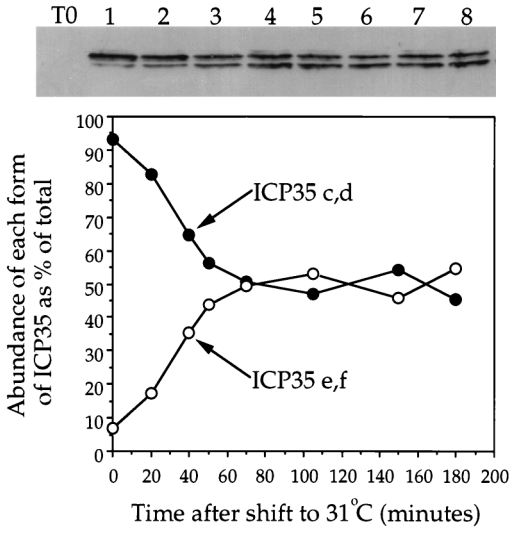

FIG. 3. Kinetics of ICP35 cleavage following temperature downshift. Vero cells were infected with HSV *ts*Prot.A and incubated at 39°C for 7 h. Following cycloheximide addition and downshift to 31°C, cell extracts were prepared, separated by SDS-PAGE, blotted, and probed for ICP35 by using monoclonal antibody MCA406. At the top of the figure is the Western blot, with lanes 1 to 8 corresponding to time at 31°C, namely, 0, 20, 40, 50, 70, 105, 150, and 180 min, respectively. Lane T0; cell extract prepared immediately postinfection. The graph represents a densitometric analysis of the data, showing changes in the percentage of ICP35 present in the uncleaved (ICP35c,d) and cleaved (ICP35e,f) form with time.

able to mature to infectivity upon temperature downshift and that the maturation of synchronized *ts*Prot.A may be used to model events occurring during a normal, nonsynchronous infection.

We next used this assay system to determine the kinetics of synchronous PFU production and to compare PFU yields with those of a wild-type HSV infection over the same time course. As expected, wild-type HSV replication proceeded at 39°C, but following cycloheximide addition, there was little or no further increase in PFU upon prolonged incubation at 31°C (Fig. 2A). In contrast, no new *ts*Prot.A PFU were generated during the 39°C incubation. Following downshift from 39°C, there was a lag period in which no new *ts*Prot.A PFU were produced (typically 40 to 50 min [Fig. 2 and data not shown]). There was then a 3-log-unit increase in PFU between 40 and 140 min of downshift, followed by a slow twofold rise in infectivity over the next 7 h. Like the initial rapid burst of PFU, the slowly maturing population resulted from consumption of preexisting polypeptides because (i) the levels of ICP35 synthesis and cleavage did not significantly increase over this time period (see below), (ii) the concentrations of cycloheximide used totally abolish de novo PFU production (Fig. 1), and (iii) infected cells returned to nonpermissive conditions after 2 h at 31°C demonstrated a similar slow increase (data not shown). The results of these experiments suggest that temperature-arrested *ts*Prot.A virions can mature to infectivity in a single, near-synchronous wave, and for the first time, the kinetics of this process have been measured. We have obtained similar results with COS7 and HepG2 cells (data not shown).

Kinetics of ICP35 cleavage and DNA packaging following recovery of *ts*Prot.A from temperature arrest. Since maturation to infectivity occurred with rapid and near-synchronous kinetics, we anticipated that these conditions could also be used to monitor the biology of earlier steps in viral assembly. We therefore examined two key events in viral maturation: the processing of ICP35c,d to ICP35e,f and packaging of DNA into the viral capsid. Earlier studies using mutant *ts*1201, which initially demonstrated that these events can occur after downshift, were principally concerned with single time points at extended periods (4 to 8 h) after return to the permissive temperature (1, 2, 29).

Vero cells were infected with *ts*Prot.A, incubated at 39°C for 7 h, and then downshifted to 31°C in the presence of cycloheximide. Extracts were prepared at particular times and then subjected to SDS-PAGE and Western blotting to monitor cleavage of ICP35c,d to ICP35e,f (Fig. 3). Approximately 7% of total cellular ICP35c,d was cleaved by the end of the 39°C incubation, but upon temperature downshift, the level increased to about 50% over the next 80 min. Little or no further cleavage occurred, even when incubation was continued for another 14 h at the permissive temperature (data not shown).

Since it is unclear what proportion of total ICP35 is encapsidated, these data do not permit us to determine the kinetics with which large-cored B capsids mature to small-cored B capsids. Nevertheless, since encapsidated ICP35 is thought to be cleaved at the same rate as unencapsidated ICP35 (9, 30), we conclude from these data that it requires about 26 min to

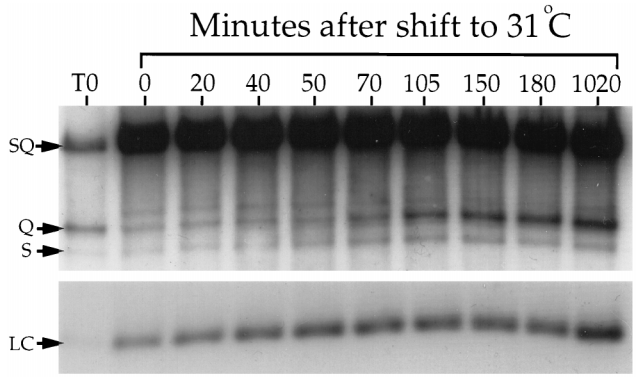

FIG. 4. Kinetics of synchronized DNA packaging. Vero cells were infected and incubated exactly as described in the legend to Fig. 3. At the indicated times after downshift to 31°C, total DNA was prepared, digested with *Bam*HI, separated on a 1.0% agarose gel, blotted to a nylon membrane, and hybridized to a mixed ^{32}P-labelled probe corresponding to the SQ cleavage junction and to a region within the UL22 gene. The full-length SQ fragment (derived from an internal duplication of the SQ-containing region and from uncleaved concatamers) and the S and Q terminal fragments are indicated by arrows. A different exposure of the region of the filter bearing the UL22 loading control fragment (LC) is shown at the bottom of the figure. Lane T0, cell extract prepared immediately postinfection.

process half of the total cleavable, encapsidated ICP35c,d under these conditions.

We next tested the kinetics of DNA packaging (Fig. 4). Packaging is tightly coupled to cleavage of head-to-tail concatameric viral DNA to genome-length pieces, generating discrete termini (33). *Bam*HI digestion of packaged DNA releases these termini, known as S and Q fragments, which can be detected following Southern blotting and hybridization with a radiolabelled probe bridging the site of cleavage (34). Unpackaged DNA is endless and does not generate these terminal *Bam*HI fragments. We prepared *Bam*HI-digested DNA from *ts*Prot.A-infected cells at different times after temperature downshift and subjected it to agarose gel electrophoresis. After Southern blotting, the filter was hybridized with a mixed radiolabelled probe to detect not only S and Q fragments but also a *Bam*HI fragment derived from the UL22 gene. The abundance of the UL22-derived fragment should remain constant following temperature downshift and provides a control for variations in DNA recovery between samples. Figure 4 shows the production of the S and Q terminal fragments with time and a different exposure of the UL22 region (LC). For up to 70 min after return to the permissive temperature, the abundance of cleaved DNA was comparable to that present immediately after infection (lane T0) and presumably derives from residual input virus. Packaging appeared to initiate by approximately 70 min of downshift and was complete by 105 to 150 min. No additional packaging took place over the next 14 h. Taking Fig. 3 and 4 together, it appears as though the wave of DNA packaging did not initiate until all of the cleavable ICP35c,d had been processed.

Intracellular trafficking of maturing HSV particles. We used indirect immunofluorescence microscopy to examine intracellular trafficking of HSV during this synchronized wave of assembly (Fig. 5). To monitor trafficking and capsid maturation, we used monoclonal antibodies 6F10 and 8F5 which recognize distinct epitopes on the major capsid protein VP5. The 6F10 antibody binds to the surfaces of large-cored B capsids and apparently all downstream assembly intermediates. In contrast, the hexon-specific 8F5 epitope (39) is efficiently displayed only after ICP35 cleavage (21, 23).

Vero cells infected with wild-type HSV strain SC16 and grown for 7 h at 39°C displayed substantial immunoreactivity to both antibodies (Fig. 5C and D). All of this staining is HSV specific, since it is absent in mock-infected cells incubated under identical conditions (Fig. 5A and B). As expected, *ts*Prot.A-infected cells incubated at 39°C displayed the 8F5 epitope poorly (Fig. 5H), despite the presence of substantial levels of 6F10 immunoreactivity (Fig. 5G). Failure to present the 8F5 epitope was a consequence of the *ts* lesion within *ts*Prot.A, because the epitope was detectable as dispersed nuclear staining in cells grown at the permissive temperature of 36°C (Fig. 5F). In this study, wild-type-virus-infected cells displayed more cytoplasmic reactivity to 6F10 than did *ts*Prot .A-infected cells grown at 36°C (compare Fig. 5C and E); however, this reactivity was somewhat variable between experiments (data not shown). Both wild-type-virus-infected (Fig. 5C) and *ts*Prot.A-infected cells incubated at either the permissive (Fig. 5E) or nonpermissive (Fig. 5G) temperature displayed a diffuse nuclear 6F10 immunoreactivity. However, mutant-virus-infected cells also contained a bright punctate pattern of nuclear 6F10 staining (Fig. 5E and G).

We monitored the appearance and intranuclear distribution of the 8F5 epitope following temperature downshift to 31°C. Immediately at the end of the 39°C block, the epitope was faintly visible within punctate structures resembling those reactive to 6F10 (compare Fig. 5G and H). Twenty minutes after downshift, the staining pattern appeared largely unchanged (Fig. 5I), but 40 min after downshift, 8F5 immunoreactivity was more readily detectable and had adopted a diffuse staining pattern throughout the nucleus, with occasional bright punctate peripheral staining (Fig. 5J). No substantial change in the intranuclear distribution of the 8F5 epitope was observed at later time points, but an increasing amount of extranuclear antigen began to appear. Cytoplasmic antigen was most easily detected after 2 or 2.5 h of incubation at 31°C (Fig. 5K and L). In serial confocal sections, we found this punctate extranuclear 8F5 staining to be evenly distributed throughout the cell body (data not shown).

Ultrastructural analysis during a wave of HSV assembly. To better understand the generation and distribution of maturing capsids, we analyzed virion assembly by electron microscopy. As shown in Fig. 6A, samples fixed at the end of the 39°C block contained clusters of capsids at the nuclear periphery, as previously reported for strain *ts*1201 (29). Occasionally, discrete capsids were observed at more interior nuclear locations (data not shown), but no cytoplasmic capsids were observed. As expected, all capsids appeared to be of the large-cored type (Fig. 6B). We then examined cells which had been incubated at the permissive temperature for 2 h (Fig. 6C to J). At this time point we have shown that infected cells contain dispersed 8F5-reactive nuclear capsids, occasional bright 8F5-reactive spots (usually close to the nuclear periphery), and cytoplasmic 8F5 reactivity (Fig. 5L). As shown in Fig. 6C to E, at this same time point peripheral nuclear clusters contained small-cored B capsids and C capsids. These clusters were often found in the vicinity of budding C capsids (Fig. 6E, left arrow) or next to distortions in the nuclear membrane (Fig. 6H). Small-cored B and C capsids were also seen as discrete, dispersed capsids throughout the interior of the nucleus (data not shown), as reported after long periods of temperature downshift (4 h) in strain *ts*1201 (29).

We frequently observed capsids which appeared to be budding through both nuclear membranes simultaneously (Fig. 6E and F). Occasionally we observed extranuclear capsids still associated with the outer nuclear membrane (Fig. 6G). These capsids appear to be enveloped, tegumented C capsids, com-

pletely enclosed by a lipid membrane and still tethered to the outer nuclear membrane by a stalk (indicated by an arrow). Enveloped and naked capsids were also readily detectable in the cytoplasm at this time point. A naked cytoplasmic C capsid, adjacent to the nuclear envelope, is indicated by an arrowhead at the extreme left of Fig. 6H. Figure 6I shows a number of naked cytoplasmic capsids, and Fig. 6J is an expansion of this region of the cytoplasm. These capsids lack the surrounding electron-dense layer of tegument visible on budding virions (Fig. 6F).

Generation of the maturing viral particles visible in Fig. 6C to J was dependent upon release of the temperature block. If infected cells were not downshifted to the permissive temperature at the end of 7 h but were maintained at 39°C for another 2 h, capsids remained in the large-cored B state (Fig. 6L). Examination of greater than 20 infected-cell sections revealed no budding capsids and a single example of a possible cytoplasmic capsid (indicated with an arrow in Fig. 6K). Consistent with these observations, no detectable levels of ICP35c,d cleavage, DNA packaging, or PFU production were found to have occurred in cells incubated at 39°C for 9 h (data not shown). Nevertheless, all of these events resumed upon downshift to the permissive temperature (data not shown).

DISCUSSION

A powerful tool in the study of complex biological phenomena is the ability to monitor the fate of a discrete, synchronized population of molecules, organelles, or cells. One common means of achieving this is to use a thermoreversible block to accumulate a population at a discrete stage in its biogenesis and then to release it as a synchronous wave. This approach has proven useful in the study of phenomena as diverse as protein trafficking through the secretory pathway (15, 31), endocytosis (36), control of the cell cycle (3), and pseudorabies virus capsid assembly (16, 17). Here we show that a thermoreversible mutation in the UL26 protease can be used to accumulate a population of immature HSV capsids and that following release of the block, the virus rapidly and efficiently matures to infectivity in a single synchronous wave. We have monitored capsid scaffold cleavage, DNA packaging, acquisition of infectivity, and intracellular trafficking in order to demonstrate the efficacy of this system and to begin a kinetic analysis of events in HSV assembly.

Upon release of the accumulated population, ICP35c,d cleavage begins immediately and reaches its maximum value of 50% processing within 60 to 70 min. It is unclear why cleavage of ICP35c,d does not proceed to completion, but this is also the case in wild-type virus infections, where approximately 50% of a pulse-labelled population of ICP35c,d remained uncleaved after 4 to 5 h of chase (32, 42). The 70-min delay between temperature downshift and initiation of DNA packaging correlates well with the time required to fully complete scaffold cleavage and is distinct from the 2-h lag seen in *ts* packaging mutants which must synthesize new polypeptides before packaging can resume (35). Once packaging had initiated, it appeared to be essentially complete within 35 min (105 min after downshift).

Infectious virion production could be detected as early as 60 min after downshift (Fig. 2) and then increased by about 2 log units over the next 80 min. An approximately twofold increase took place over the next 6 h. Of the total yield of infectious virions, 80% were generated after 105 min of downshift (by which time most DNA packaging had been completed [Fig. 4]). This close correspondence between the kinetics of packaging and PFU production suggests that newly formed C capsids very rapidly proceed to acquire infectivity. Although it is tempting to speculate that the data in Fig. 2 define the kinetics of capsid envelopment, the nature of the rate-limiting step for acquisition of HSV infectivity is not known. In principle, this study could be timing the processing of a critical viral polypeptide or even the delivery of mature virions to a compartment from which they are efficiently released upon cell breakage. Availability of this assay system should now make it possible to address such issues in the future.

A striking result was the sudden appearance of dispersed 8F5-reactive nuclear antigen between 20 and 40 min after downshift to the permissive temperature. The monoclonal antibody 8F5 has been shown to recognize a conformational epitope displayed by the major capsid protein VP5 when present within hexons (39). Furthermore, display of this epitope occurs efficiently only in the context of the maturing capsid: 8F5 reacts poorly with nuclear VP5 when capsid assembly is blocked or slowed upstream of ICP35 cleavage by deletion of UL26 or ICP35 (11, 21). The increase in intensity of nuclear 8F5 antigen upon temperature downshift may therefore measure the rate at which VP5 assembles into this hexon-specific conformation. The hexon-specific conformation was inefficiently displayed by 20 min after downshift, when only about 17% of ICP35c,d had been cleaved to the mature form, but was readily visible by 40 min after downshift when about 35% of the ICP35c,d had been cleaved.

The pattern of 6F10 immunoreactivity was distinct from that of wild type, even at the permissive temperature. Although both wild-type- and mutant-virus-infected cells displayed diffuse 6F10 nuclear reactivity, mutant-virus-infected cells also contained bright punctate staining, commonly at the nuclear periphery and showing some resemblance to assemblons, as defined by Ward and coworkers (41). It remains to be determined whether this punctate VP5 staining is directly related to the properties of the *ts* UL26 allele and what significance these structures have for viral assembly.

By about 2 to 2.5 h of temperature downshift, when 30 to 60% of virions had acquired infectivity, 8F5-reactive antigen was visible in the extranuclear regions of the cells (Fig. 5K and L). It is known that the 8F5 antibody does not bind unassembled VP5 (39) and that 8F5 fails to recognize extranuclear VP5 when capsid maturation is rendered inefficient by ICP35 deletion, despite it being readily detectable in the cytoplasm and nucleus when stained with other anti-VP5 antibodies (21). Because of this, we speculate that the cytoplasmic 8F5 staining visible in our study could represent matured HSV capsids (singly or in aggregates) which have trafficked from the cell nucleus. As would be expected, 8F5 antigen is readily detectable in the cytoplasm during a wild-type virus infection conducted at 39°C (Fig. 5D). Further studies will be necessary to properly characterize the nature and location of this cytoplasmic hexon-associated antigen.

Our ultrastructural analyses were consistent with the kinetics of ICP35c,d cleavage, DNA packaging, acquisition of infectivity, and intracellular trafficking of VP5. Immediately after the end of the 39°C block, when only very low levels of ICP35 cleavage had occurred, nuclei contained only large-cored B capsids. These capsids were present in aggregates as previously reported (29), and no capsids were observed in the cytoplasm. Following 2 h of incubation at the permissive temperature (time sufficient for completion of scaffold cleavage and most or all DNA packaging), capsid aggregates were found to contain small-cored B capsids and packaged C capsids. Packaged C capsids could also be seen budding through both nuclear membranes, and naked C capsids could be observed within the cytoplasm.

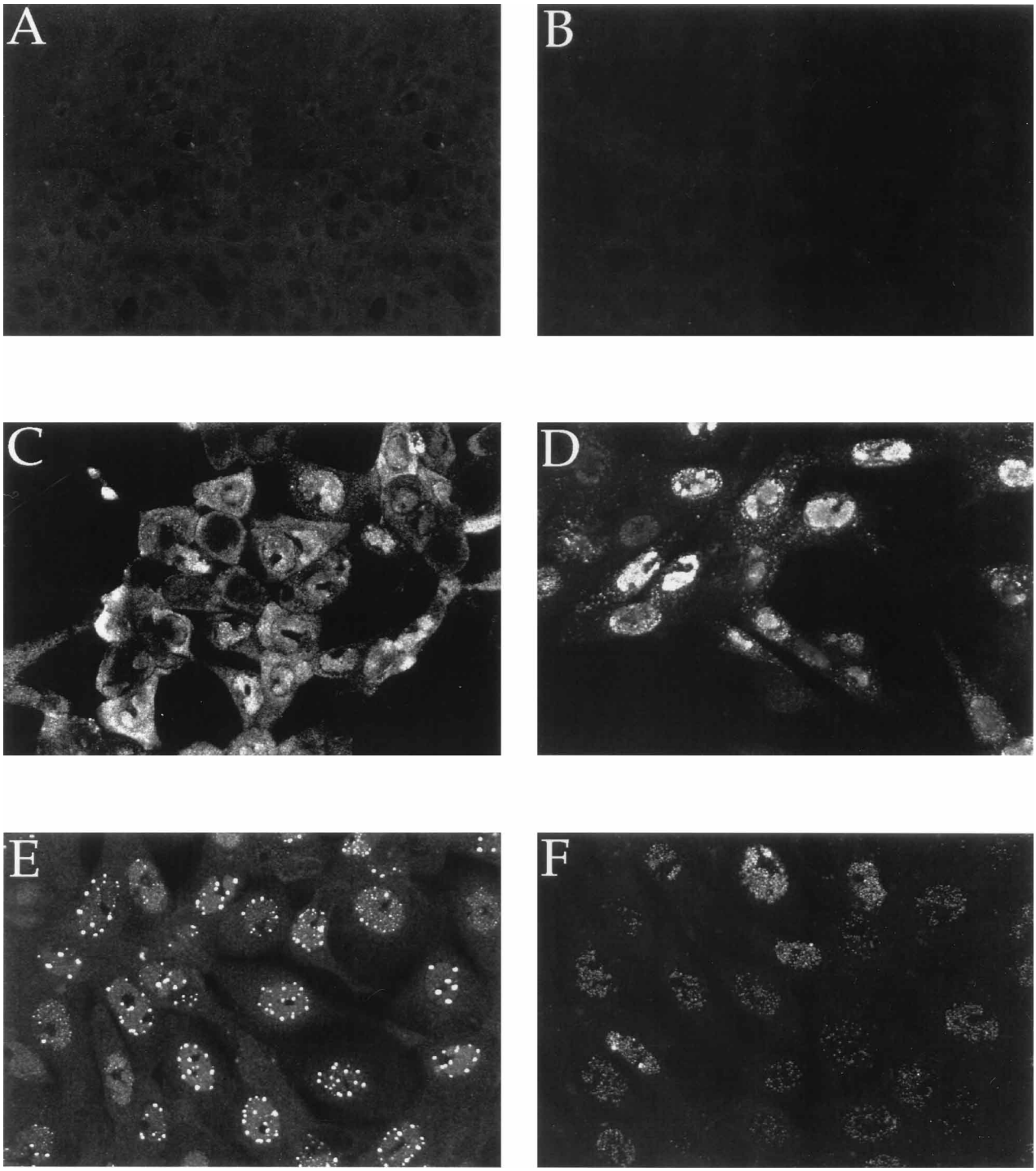

FIG. 5. Intracellular redistribution of maturing HSV capsids during a single wave of assembly. Vero cells were mock infected (A and B) or infected with SC16 (C and D) or with *ts*Prot.A (E to L) and then incubated at 36°C (E and F) or 39°C (all other samples) for 7 h. Samples were then either fixed and processed immediately (A to H) or first incubated at 31°C in the presence of cycloheximide for 20 min (I), 40 min (J), 120 min (K), or 150 min (L). After fixation, cells were made permeable and incubated with anti-VP5 monoclonal antibody 6F10 (A, C, E, and G) or 8F5 (B, D, F, and H to L). Arrowheads in panel K point to extranuclear capsid antigen.

Budding through and pinching off of both nuclear membranes (Fig. 6E and F) could result in the formation of an enveloped virion within a outer lipid vesicle, as in Fig. 6G. Upon detachment, these vesicles could deliver enveloped particles to later stages of the secretory pathway, a model similar to that proposed by Harson and Grose for varicella-zoster virus (14). Alternatively, these structures might be an important intermediate in virion de-envelopment, since they provide an effective way of bringing the outside surface of the envelope and the inner surface of the outer nuclear membrane into intimate contact over a large surface area. This close apposition of the entire envelope surface with the outer

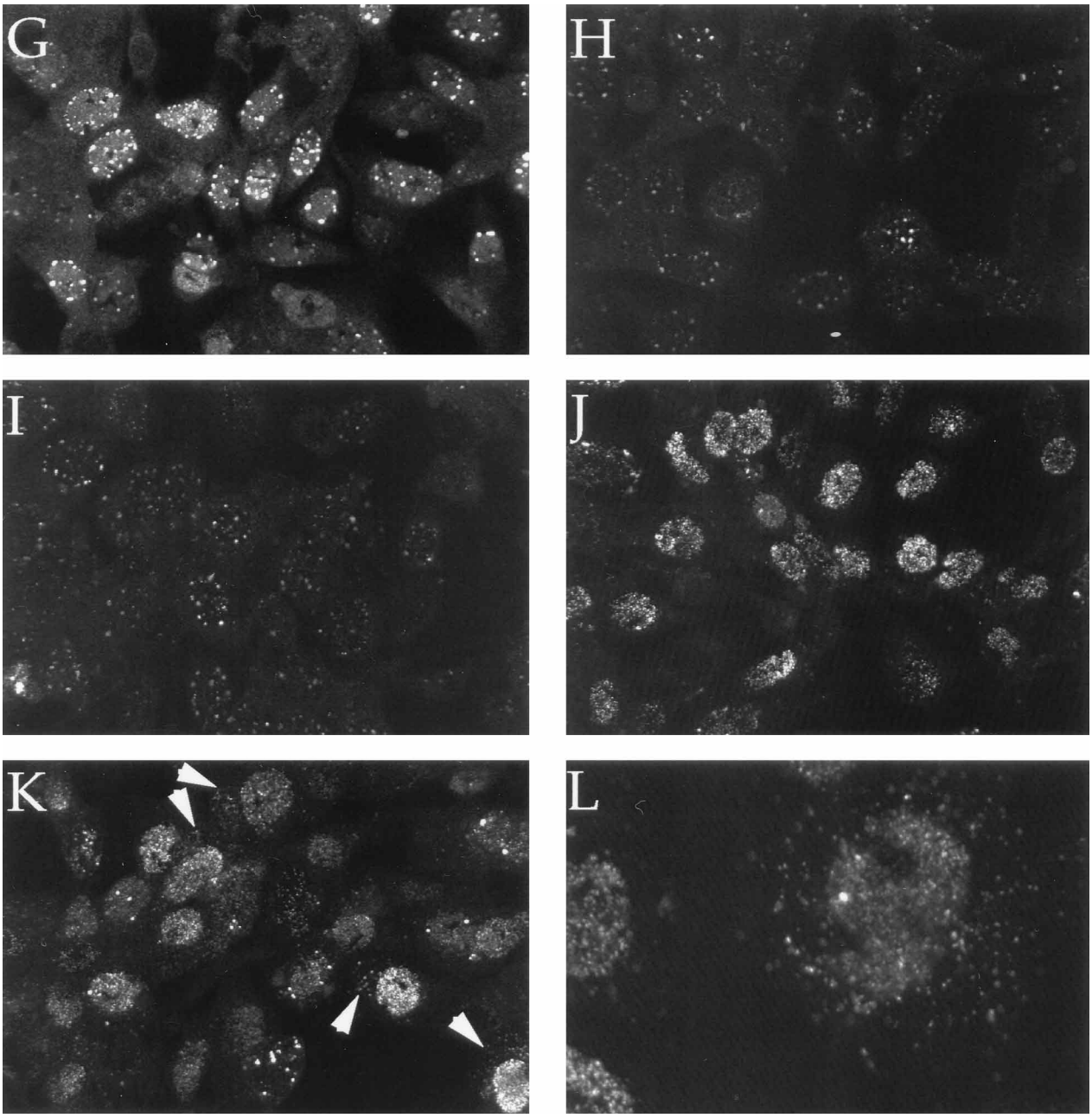

FIG. 5—*Continued.*

nuclear membrane and the high degree of curvature imposed upon the two membranes could combine to facilitate fusion of the bilayers and entry of naked capsids into the cytoplasm. If fusion were possible only under these circumstances, it would remove any likelihood of spurious and harmful fusion events between the inner and outer nuclear membranes.

A unique feature of our microscopic analyses is that we are able to impose narrow limits upon the age of any matured particles which we observe. All of the packaged virions in Fig. 6C to J must have matured from large-cored B capsids in the preceding 2 h. Further, since extranuclear C capsids were not seen in ultrastructural analyses after 60 min at 31°C (data not shown) and since packaging did not initiate until approximately 70 min after downshift (Fig. 4), we think it likely that most of the enveloped or naked extranuclear capsids in Fig. 6G to J are no more than 50 to 60 min old. This places an upper limit on the time required to bud through both nuclear membranes and to travel into the cytoplasm. The ready detection of naked cytoplasmic capsids at this time point also suggests that newly enveloped capsids are able to very rapidly de-envelope upon leaving the nucleus. This finding excludes the possibility that de-envelopment into the cytoplasm occurs only after enveloped particles have persisted in an infected-cell cytoplasm for many hours. Quantitative electron microscopy at more-frequent time points during a synchronous release should now make it possible to precisely time and order each of the events in assembly and trafficking.

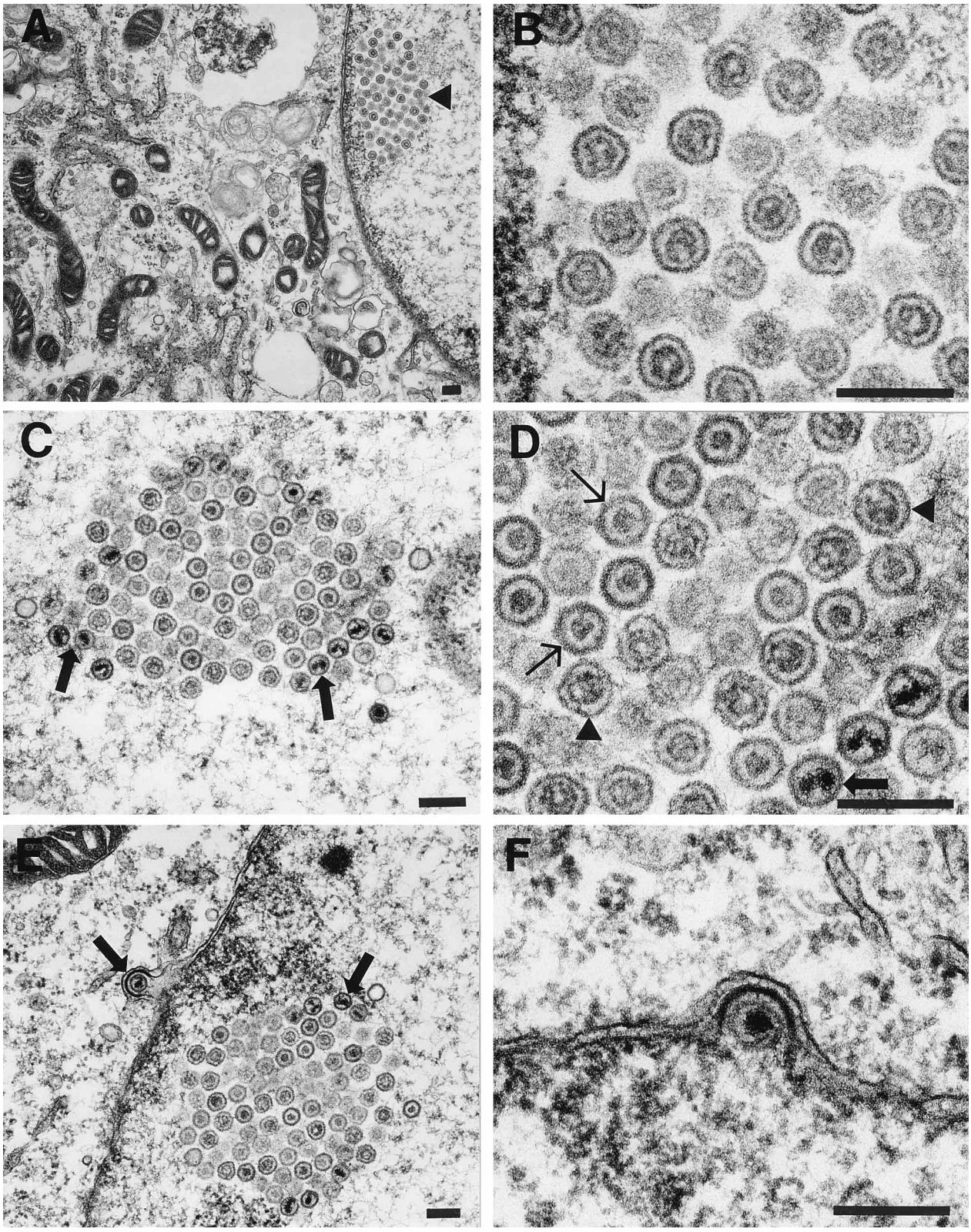

FIG. 6. Ultrastructural analysis following temperature downshift. Vero cells were infected with *ts*Prot.A and then incubated for 7 h at 39°C, and cycloheximide was added. Samples were processed for electron microscopy immediately (A and B) or following 2 h of incubation at 31°C (C to J) or 39°C (K and L). Capsids are indicated by arrowheads (large-cored B capsids), thin arrows (small-cored B capsids), or thick arrows (C capsids). Bars, 200 nm. (A) Cluster of capsids adjacent to the inner surface of the nuclear membrane (arrowhead). No capsids are visible in the cytoplasm. (B) Higher-magnification image of the cluster in panel A showing that capsids appear to be of the large-cored B type. (C and D) Maturing capsid cluster shown at two different magnifications, containing large- and small-cored B capsids and peripheral C capsids. (E) Capsid cluster similar to that in panel C, with a packaged C capsid budding through both nuclear membranes (left arrow). (F) Nuclear C capsid budding through both inner and outer nuclear membranes. (G) Enveloped C capsid within a sealed vesicle anchored to the surface of the nuclear membrane by a stalk

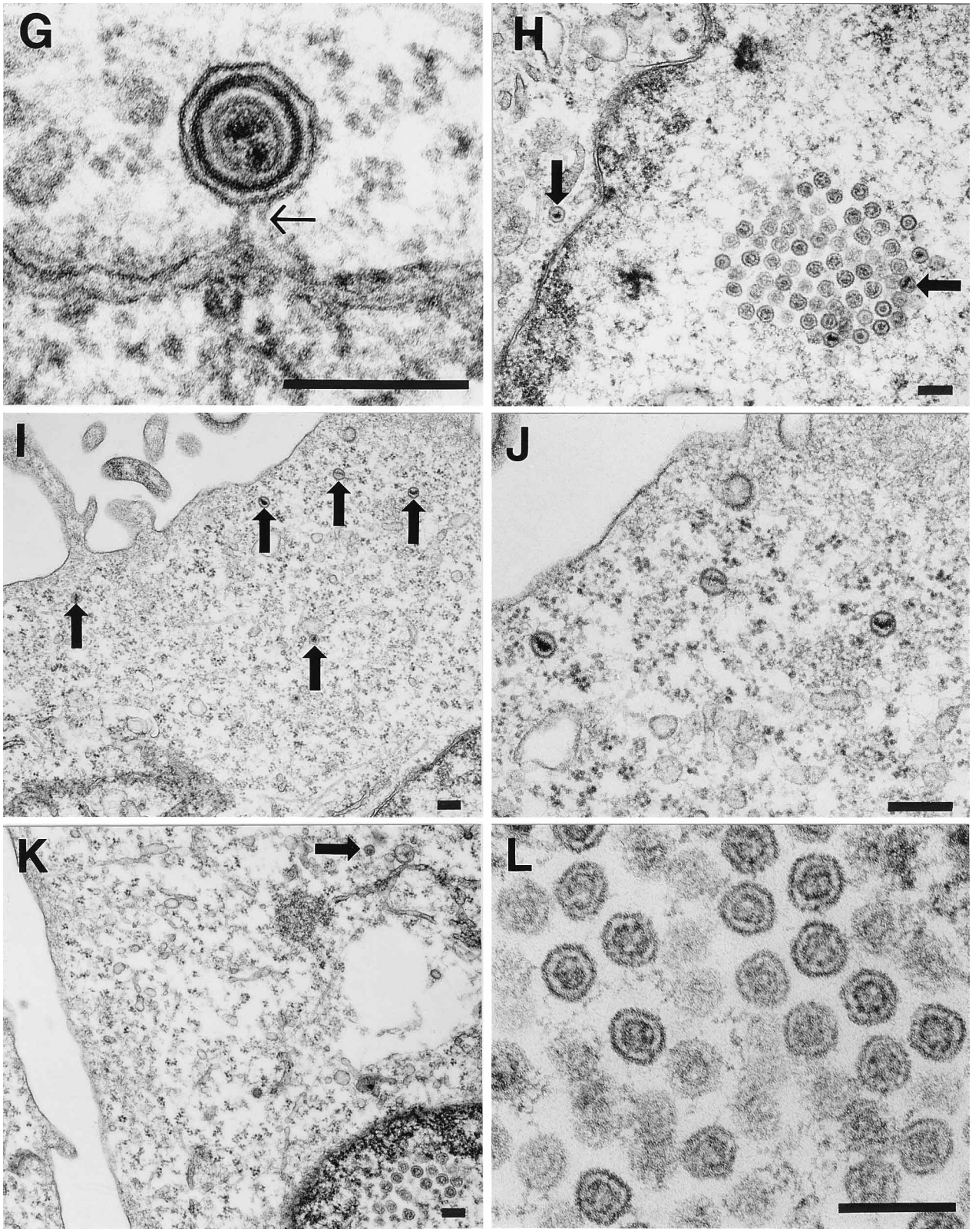

(arrow). (H) Capsid cluster similar to that in panels C and E. A naked C capsid (left arrow) is visible in the cytoplasm adjacent to the nuclear membrane. (I) Cytoplasm lying between nuclear rim (bottom right corner) and plasma membrane. Several naked C capsids are visible (arrows). (J) Higher-magnification image of three capsids from the top right of panel I. (K) Rare example of a naked capsid in cytoplasm of cells maintained at the nonpermissive temperature. (L) Capsids in cells held at the nonpermissive temperature maintain the large-cored B phenotype.

ACKNOWLEDGMENTS

This work was supported by grants to D.W.W. from the National Institutes of Health (AI-38265) and the American Federation for Medical Research and by Cancer Center grant P30-CA13330. G.A.C. was supported by National Institutes of Health training grant T32 GM07491.

We thank Lily Huang for excellent technical assistance and gratefully acknowledge the Analytical Imaging Facility of the Albert Einstein College of Medicine for help with electron and confocal microscopy. We thank Margaret Kielian, Dennis Shields, and Sandra Weller for helpful discussions and comments on the manuscript.

REFERENCES

1. **Addison, C., F. J. Rixon, and V. G. Preston.** 1990. Herpes simplex virus type 1 UL28 gene product is important for the formation of mature capsids. J. Gen. Virol. **71:**2377–2384.
2. **al-Kobaisi, M. F., F. J. Rixon, I. McDougall, and V. G. Preston.** 1991. The herpes simplex virus UL33 gene product is required for the assembly of full capsids. Virology **180:**380–388.
3. **Bernander, R., T. Akerlund, and K. Nordstrom.** 1995. Inhibition and restart of initiation of chromosome replication: effects on exponentially growing *Escherichia coli* cells. J. Bacteriol. **177:**1670–1682.
4. **Braun, D. K., B. Roizman, and L. Pereira.** 1984. Characterization of post-translational products of herpes simplex virus gene 35 proteins binding to the surfaces of full capsids but not empty capsids. J. Virol. **49:**142–153.
5. **Browne, H., S. Bell, T. Minson, and D. W. Wilson.** 1996. An endoplasmic reticulum-retained herpes simplex virus glycoprotein H is absent from secreted virions: evidence for reenvelopment during egress. J. Virol. **70:**4311–4316.
6. **Campadelli-Fiume, G., F. Farabegoli, S. Di Gaeta, and B. Roizman.** 1991. Origin of unenveloped capsids in the cytoplasm of cells infected with herpes simplex virus 1. J. Virol. **65:**1589–1595.
7. **Casjens, S., and J. King.** 1975. Virus assembly. Annu. Rev. Biochem. **44:** 555–611.
8. **Davison, M. D., F. J. Rixon, and A. J. Davison.** 1992. Identification of genes encoding two capsid proteins (VP24 and VP26) of herpes simplex virus type 1. J. Gen. Virol. **73:**2709–2713.
9. **Desai, P., S. C. Watkins, and S. Person.** 1994. The size and symmetry of B capsids of herpes simplex virus type 1 are determined by the gene products of the UL26 open reading frame. J. Virol. **68:**5365–5374.
10. **Di Lazzaro, C., G. Campadelli-Fiume, and M. R. Torrisi.** 1995. Intermediate forms of glycoconjugates are present in the envelope of herpes simplex virions during their transport along the exocytic pathway. Virology **214:**619–623.
11. **Gao, M., L. Matusick-Kumar, W. Hurlburt, S. F. DiTusa, W. W. Newcomb, J. C. Brown, P. J. McCann, I. Deckman, and R. J. Colonno.** 1994. The protease of herpes simplex virus type 1 is essential for functional capsid formation and viral growth. J. Virol. **68:**3702–3712.
12. **Gershon, A. A., D. L. Sherman, Z. Zhu, C. A. Gabel, R. T. Ambron, and M. D. Gershon.** 1994. Intracellular transport of newly synthesized varicella-zoster virus: final envelopment in the *trans*-Golgi network. J. Virol. **68:**6372–6390.
13. **Gibson, W., and B. Roizman.** 1972. Proteins specified by herpes simplex virus. VIII. Characterization and composition of multiple capsid forms of subtypes 1 and 2. J. Virol. **10:**1044–1052.
14. **Harson, R., and C. Grose.** 1995. Egress of varicella-zoster virus from the melanoma cell: a tropism for the melanocyte. J. Virol. **69:**4994–5010.
15. **Jantti, J., S. Keranen, J. Toikkanen, E. Kuismanen, C. Ehnholm, H. Soderlund, and V. M. Olkkonen.** 1994. Membrane insertion and intracellular transport of yeast syntaxin SSO2p in mammalian cells. J. Cell Sci. **107:**3623–3633.
16. **Ladin, B. F., M. L. Blankenship, and T. Ben-Porat.** 1980. Replication of herpesvirus DNA. V. Maturation of concatemeric DNA of pseudorabies virus to genome length is related to capsid formation. J. Virol. **33:**1151–1164.
17. **Ladin, B. F., S. Ihara, H. Hampl, and T. Ben-Porat.** 1982. Pathway of assembly of herpesvirus capsids: an analysis using DNA+ temperature-sensitive mutants of pseudorabies virus. Virology **116:**544–561.
18. **Liu, F., and B. Roizman.** 1992. Differentiation of multiple domains in the herpes simplex virus 1 protease encoded by the UL26 gene. Proc. Natl. Acad. Sci. USA **89:**2076–2080.
19. **Liu, F., and B. Roizman.** 1993. Characterization of the protease and other products of amino-terminus-proximal cleavage of the herpes simplex virus 1 UL26 protein. J. Virol. **67:**1300–1309.
20. **Liu, F. Y., and B. Roizman.** 1991. The herpes simplex virus 1 gene encoding a protease also contains within its coding domain the gene encoding the more abundant substrate. J. Virol. **65:**5149–5156.
21. **Matusick-Kumar, L., W. Hurlburt, S. P. Weinheimer, W. W. Newcomb, J. C. Brown, and M. Gao.** 1994. Phenotype of the herpes simplex virus type 1 protease substrate ICP35 mutant virus. J. Virol. **68:**5384–5394.
22. **Matusick-Kumar, L., P. J. McCann III, B. J. Robertson, W. W. Newcomb, J. C. Brown, and M. Gao.** 1995. Release of the catalytic domain N_o from the herpes simplex virus type 1 protease is required for viral growth. J. Virol. **69:**7113–7121.
23. **Matusick-Kumar, L., W. W. Newcomb, J. C. Brown, P. J. McCann III, W. Hurlburt, S. P. Weinheimer, and M. Gao.** 1995. The C-terminal 25 amino acids of the protease and its substrate ICP35 of herpes simplex virus type 1 are involved in the formation of sealed capsids. J. Virol. **69:**4347–4356.
24. **Montalvo, E. A., R. T. Parmley, and C. Grose.** 1986. Varicella-zoster viral glycoprotein envelopment: ultrastructural cytochemical localization. J. Histochem. Cytochem. **34:**281–284.
25. **Newcomb, W. W., and J. C. Brown.** 1989. Use of Ar^+ plasma etching to localize structural proteins in the capsid of herpes simplex virus type 1. J. Virol. **63:**4697–4702.
26. **Newcomb, W. W., and J. C. Brown.** 1991. Structure of the herpes simplex virus capsid: effects of extraction with guanidine hydrochloride and partial reconstitution of extracted capsids. J. Virol. **65:**613–620.
27. **Penfold, M. E., P. Armati, and A. L. Cunningham.** 1994. Axonal transport of herpes simplex virions to epidermal cells: evidence for a specialized mode of virus transport and assembly. Proc. Natl. Acad. Sci. USA **91:**6529–6533.
28. **Person, S., S. Laquerre, P. Desai, and J. Hempel.** 1993. Herpes simplex virus type 1 capsid protein, VP21, originates within the UL26 open reading frame. J. Gen. Virol. **74:**2269–2273.
29. **Preston, V. G., J. A. Coates, and F. J. Rixon.** 1983. Identification and characterization of a herpes simplex virus gene product required for encapsidation of virus DNA. J. Virol. **45:**1056–1064.
30. **Preston, V. G., F. J. Rixon, I. M. McDougall, M. McGregor, and M. F. al Kobaisi.** 1992. Processing of the herpes simplex virus assembly protein ICP35 near its carboxy terminal end requires the product of the whole of the UL26 reading frame. Virology **186:**87–98.
31. **Rindler, M. J., I. E. Ivanov, H. Plesken, and D. D. Sabatini.** 1985. Polarized delivery of viral glycoproteins to the apical and basolateral plasma membranes of Madin-Darby canine kidney cells infected with temperature-sensitive viruses. J. Cell Biol. **100:**136–151.
32. **Rixon, F. J., A. M. Cross, C. Addison, and V. G. Preston.** 1988. The products of herpes simplex virus type 1 gene UL26 which are involved in DNA packaging are strongly associated with empty but not with full capsids. J. Gen. Virol. **69:**2879–2891.
33. **Roizman, B., and A. E. Sears.** 1990. Herpes simplex viruses and their replication, p. 1795–1894. *In* B. N. Fields, D. M. Knipe, et al. (ed.), Virology. Raven Press, Ltd., New York, N.Y.
34. **Shao, L., L. M. Rapp, and S. K. Weller.** 1993. Herpes simplex virus 1 alkaline nuclease is required for efficient egress of capsids from the nucleus. Virology **196:**146–162.
35. **Sherman, G., and S. L. Bachenheimer.** 1987. DNA processing in temperature-sensitive morphogenic mutants of HSV-1. Virology **158:**427–430.
36. **Silverstein, S. C., R. M. Steinman, and Z. A. Cohn.** 1977. Endocytosis. Annu. Rev. Biochem. **46:**669–722.
37. **Stackpole, C. W.** 1969. Herpes-type virus of the frog renal adenocarcinoma. I. Virus development in tumor transplants maintained at low temperature. J. Virol. **4:**75–93.
38. **Thomsen, D. R., W. W. Newcomb, J. C. Brown, and F. L. Homa.** 1995. Assembly of the herpes simplex virus capsid: requirement for the carboxyl-terminal twenty-five amino acids of the proteins encoded by the UL26 and UL26.5 genes. J. Virol. **69:**3690–3703.
39. **Trus, B. L., W. W. Newcomb, F. P. Booy, J. C. Brown, and A. C. Steven.** 1992. Distinct monoclonal antibodies separately label the hexons or the pentons of herpes simplex virus capsid. Proc. Natl. Acad. Sci. USA **89:**11508–11512.
40. **van Genderen, I. L., R. Brandimarti, M. R. Torrisi, G. Campadelli, and G. van Meer.** 1994. The phospholipid composition of extracellular herpes simplex virions differs from that of host cell nuclei. Virology **200:**831–836.
41. **Ward, P. L., W. O. Ogle, and B. Roizman.** 1996. Assemblons: nuclear structures defined by aggregation of immature capsids and some tegument proteins of herpes simplex virus 1. J. Virol. **70:**4623–4631.
42. **Weinheimer, S. P., P. J. McCann, D. R. O'Boyle, J. T. Stevens, B. A. Boyd, D. A. Drier, G. A. Yamanaka, C. L. DiIanni, I. C. Deckman, and M. G. Cordingley.** 1993. Autoproteolysis of herpes simplex virus type 1 protease releases an active catalytic domain found in intermediate capsid particles. J. Virol. **67:**5813–5822.
43. **Whealy, M. E., J. P. Card, R. P. Meade, A. K. Robbins, and L. W. Enquist.** 1991. Effect of brefeldin A on alphaherpesvirus membrane protein glycosylation and virus egress. J. Virol. **65:**1066–1081.